JOURNAL OF MATERIALS SCIENCE 30 (1995) 1698–1708

Effect of alloying elements and dendrite arm spacing on the microstructure and hardness of an Al–Si–Cu–Mg–Fe–Mn (380) aluminium die-casting alloy

A. M. SAMUEL, F. H. SAMUEL
Département des Sciences Appliquées, Université du Québec à Chicoutimi, 555, boulevard de l'Université, Chicoutimi, Québec, Canada G7H 2B1

The microstructure of aluminium alloys based on 380 die-casting alloy was studied in detail, as a function of the alloying elements iron, magnesium, copper and manganese, and the solidification rate. Three methods of solidification were employed to simulate cooling rates obtained from investment, permanent, and die-casting processes, corresponding to ~ 0.4, ~ 12 and $\sim 260\,^{\circ}C\,s^{-1}$, respectively, with emphasis on the highest cooling rate. Hardness measurements were carried out on samples obtained from the latter, in the as-cast and T5 tempered conditions (4 h at 25, 155, 180, 200 and 220 °C). The results have been discussed and the correlation between the hardness and microstructure as a function of alloying elements is presented. The effect of solution heat treatment on the variations in the microstructure and hardness has also been discussed.

1. Introduction

The 380 family of Al–Si–Cu alloys is perhaps the most widely used aluminium-base alloy system in die casting, the properties of these ternary alloys representing the best compromise between their component Al–Si and Al–Cu binary alloy systems, and consequently, an optimum combination of foundry characteristics [1, 2].

A knowledge of the effect of compositional variation upon the mechanical properties has been one of the principal concerns of die casters, and to this end, several studies have been carried out over the years to determine the influence of both alloying elements and impurities on these die-casting alloys [2–6]. Today, the effect of various elements on the mechanical properties can be predicted with reasonable accuracy. Whether an element acts as an alloying element or an impurity is, however, not easy to define, as it may have both useful and adverse effects. Most of these studies have shown that the two main elements that give cause for concern are iron and magnesium, where excess amounts of the first can deleteriously affect the mechanical properties, whereas excess of the latter improves the strength of the alloy but simultaneously reduces its ductility and impact properties [3, 6–9].

In an earlier publication, the effect of alloying elements on the solidification characteristics of 380 die-casting alloy was investigated in detail [10]. However, the experimental apparatus used produced cooling rates far below those observed in a typical die-casting process. This was attempted in the present study with the use of a melt-quenching technique, and resulted in producing solid disc-like pellets that possessed very fine microstructures and gave dendrite arm spacings of the order of 4–6 μm, corresponding to the high cooling rates prevalent in die casting. Specimens were prepared from these pellets and microstructurally examined, and their hardness values determined. The effect of alloy composition and related microstructural characteristics on the hardness of the alloy are presented.

2. Experimental procedure

The base 380 alloy was supplied by Alcan Ingot Alloys Canada (Guelph, Ontario), with the chemical composition shown in Table I. The alloy was supplied in the unmodified form. About 6 kg base material were remelted at a time, and to each melt, measured quantities of various alloying elements such as iron, magnesium, copper and manganese were added in the form of master alloys to obtain the final compositions shown in Table II.

The melts were degassed at 740 °C for 20 min by passing dry argon through a lance. The hydrogen level of the melt after degassing was determined to be 0.14 ml/100 g Al, using an Alscan™ hydrogen analyser. No melt treatment, i.e. modification, was applied. The degassed materials were variously poured into:

(a) a graphite mould of 5 cm diameter maintained at 400 °C, which was expected to produce cooling rates close to those obtained in investment castings ($\sim 0.4\,^{\circ}C\,s^{-1}$);

0022–2461

TABLE I Chemical composition of the as-received 380 base alloy

	Cu	Fe	Mg	Mn	Si	Ti	Zn	Ni	Cr	Al
Specified conc. (wt %)	3.00–4.00	1.00–1.30	0.10	0.50	7.50–9.50	–	3.00	–	–	Bal.
Chemical analysis (wt %)	3.22	1.01	0.06	0.16	9.18	0.02	2.28	0.04	0.03	Bal.

TABLE II Chemical composition of the as-cast 380 alloys

380 Alloy type	Elements (wt %)						
	Cu	Fe	Mg	Mn	Zn	Others	Al
Base alloy	3.22	1.01	0.06	0.16	2.28	As in Table I	Bal.
Mn-containing	3.22	1.01	0.06	0.46	2.28	As in Table I	Bal.
Fe-containing	3.22	0.76	0.06	0.16	2.28	As in	Bal.
	3.22	1.50	0.06	0.16	2.28	Table I	Bal.
	3.22	1.80	0.06	0.16	2.28		Bal.
Mg-containing	3.22	1.01	0.23	0.16	2.28	As in	Bal.
	3.22	1.01	0.50	0.16	2.28	Table I	Bal.
Cu-containing	3.43	1.01	0.06	0.16	2.28	As in	Bal.
	4.09	1.01	0.06	0.16	2.28	Table I	Bal.

(b) a copper mould, with a ceramic riser mounted at its top (Fig. 1), and placed in a tank of running cold water ($\sim$ 10 °C). The cooling rates achieved were close to those obtained from permanent mould castings ($\sim$ 10–15 °C s^{-1});

(c) cold water directly, to form discs, roughly 6 mm diameter and 1.5 mm thick. This process of melt quenching has long been known to produce fine structures, with dendrite arm spacings (DAS) $\sim$ 4–6 μm [11], resembling those obtained from a typical die-casting process.

A batch of samples produced from method (c) was immediately aged at 25 (room temperature), 155, 180, 200 and 220 °C for 4 h. The hardness of these aged samples was measured using a Rockwell F hardness tester, where an average of at least ten readings was taken for each measurement.

Samples for metallographic observations were prepared from each type of casting (i.e. mounting in bakelite, followed by polishing of the surfaces). Microstructural details were analysed using optical microscopy (Olympus PMG3), while the eutectic silicon particle characteristics and dendrite arm spacings (DAS) were measured using image analysis (Leco 2001 image analysis system used in conjunction with the optical microscope). These measurements were done in the usual manner as that employed for feature measurements of any specified phase (see [12] for details). The DAS values reported are averages taken over 40–50 readings in each case.

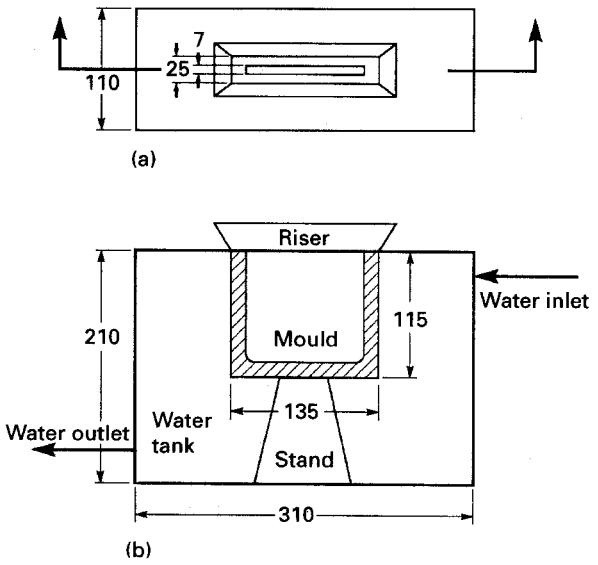

Figure 1 Experimental apparatus for water-chilled alloy castings. (a) Top view, (b) sectional view. Dimensions in millimetres.

3. Results and discussion

3.1. Cooling rate

The relationship between the dendrite arm spacing, d, and the corresponding cooling rate, $\dot{T}$, is normally described by the relation,

$$d = A(\dot{T})^n \quad (1)$$

From our earlier studies [13], A and n for the present 380 alloy are approximately 31 and -0.366, respectively (cf. the long freezing range alloy 356, where A is about 48 and n is ~ -0.4 [14]). Table III shows the expected values of cooling rate for the three methods of solidification employed in the present work, where 356 alloy (containing about 7 wt % Si) is used as reference.

3.2. Microstructures of the solidified alloys

The effect of alloying elements on the variation in the microstructure of slowly cooled materials (cooling

TABLE III Cooling rates corresponding to DAS obtained from the three methods of solidifcation used in the present work

Method	DAS (μm)	$\dot{T}$ (°C s^{-1})	
		380 alloy	356 alloy (ref. 14)
Graphite mould	40–60	0.30–0.15	1.30–0.50
Water-chilled copper mould	10–15	22–8	44–21
Melt quenching	4–6	265–90	800–255

rate $\sim 0.4\,°C\,s^{-1}$, corresponding to a DAS of ~ 50 μm) has been discussed in detail elsewhere [10]. Fig. 2 shows the microstructural refinement resulting from the increase in cooling rate, as evidenced by the difference in the primary aluminium dendrite arm spacings observed in Fig. 2a, b and c for the three methods of solidification. The high-magnification micrograph of Fig. 2d reveals the fineness of the eutectic silicon particles achieved at a cooling rate of $\sim 260\,°C\,s^{-1}$. Typical microstructures obtained at 13 and 265 °C s^{-1} are shown in Fig. 3a and b, respectively. The main constituents in Fig. 3a, apart from the eutectic silicon particles, are primary silicon (marked A), the needle-like β-iron phase (Al_5FeSi, marked B), and the Al_2Cu phase seen nucleated at the large interface of the β-needles (along their length, marked C) or else existing within the aluminium matrix. This phase occurs in the form of eutectic pockets (as fine fibres intermixed with aluminium, marked D) or as blocky/massive particles (marked E). Increasing the cooling rate to 265 °C s^{-1}, Fig. 3b, is seen to result in replacement of the needle-like β-phase by the Chinese script α-phase ($Al_{15}(Fe,Mn)_3Si_2$). Although the Al_2Cu phase is still visible in the microstructure, it is difficult to distinguish clearly between its different forms.

Below 1 wt % iron, the alloy exhibits a tendency to weld or "solder" to the die surface. Greatest freedom from welding is obtained with a 1–1.3 wt % content of iron [4]. This element helps in minimizing hot cracking and reducing shrinkage, and also acts as a grain refiner. However, in excess amount, brittleness results, with low resistance to shock and poor machinability [6]. Fluidity and casting characteristics are also seriously affected.

Fig. 4a–c demonstrate the progressive increase in both amount and maximum length of β-iron needles with increasing iron content, when the alloy cools at 10–12 °C s^{-1}. For 0.76 wt % Fe, Fig. 4a, the Chinese script α-phase (arrowed) predominates the microstructure. β-needles were observed when the iron concentration was of the order of 1 wt % (Fig. 3a) or more (Fig. 4b, c).

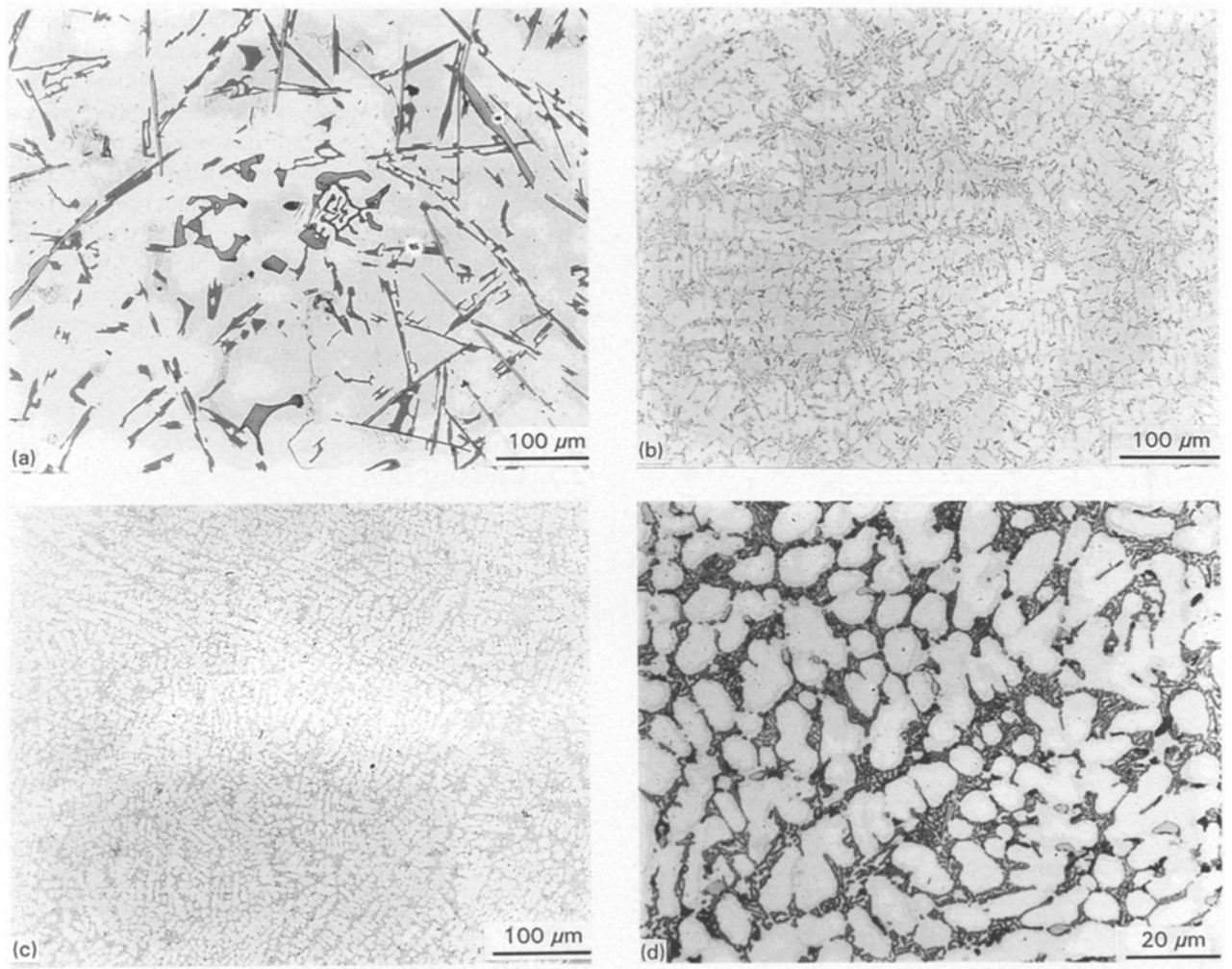

Figure 2 Microstructures of as-cast 380 base alloy: (a) DAS ~ 40–60 μm; (b) DAS ~ 10–15 μm; (c) DAS ~ 4–6 μm; (d) high-magnification micrograph of a sample of the type shown in (c).

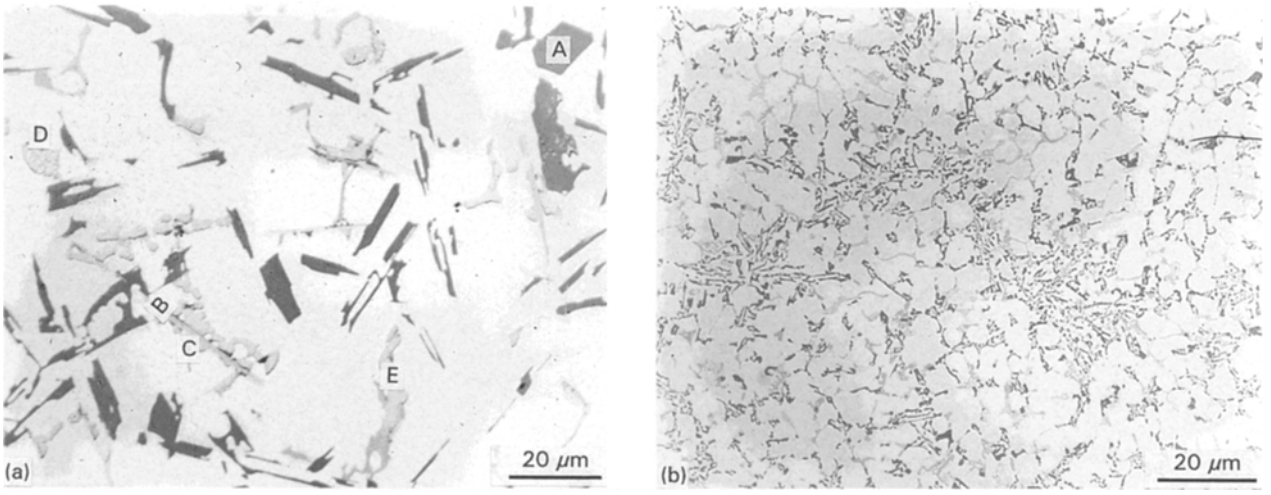

Figure 3 Microstructures of 380 alloy cooled at (a) $13\,°C\,s^{-1}$ and (b) $265\,C\,s^{-1}$.

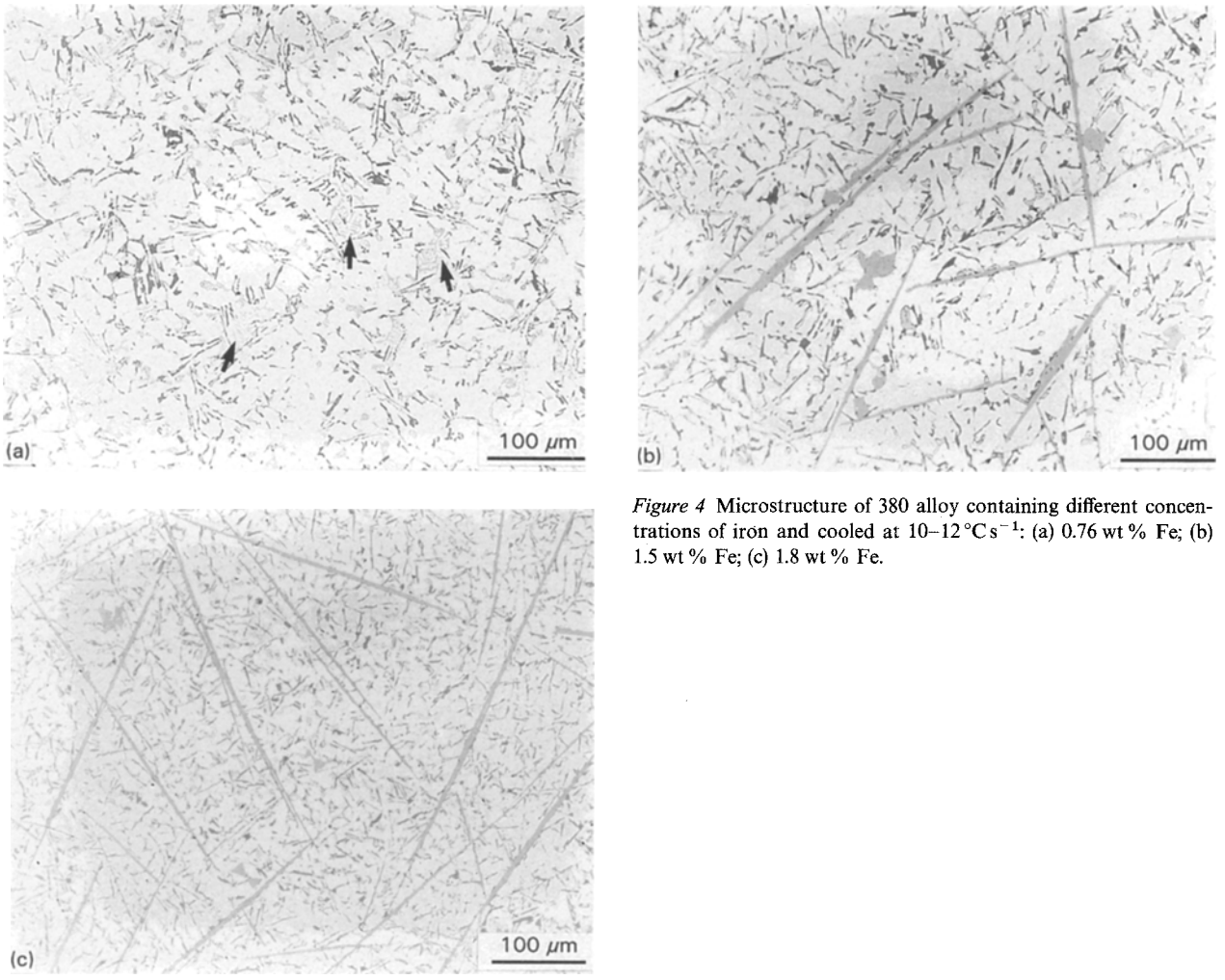

Figure 4 Microstructure of 380 alloy containing different concentrations of iron and cooled at $10–12\,°C\,s^{-1}$: (a) 0.76 wt % Fe; (b) 1.5 wt % Fe; (c) 1.8 wt % Fe.

A few scattered α-iron plates (with no traces of β-needles) were observed when the alloy containing 0.76 wt % Fe was melt quenched, Fig. 5a. Short needles of β-phase (10–20 μm) were first seen when the iron content was increased to 1.5 wt % (Fig. 5b) and became noticeable for an iron level of 1.8 wt % or above (Fig. 5c). The variation in the β-iron needle length with iron content and cooling rate (expressed in terms of the DAS) for the as-cast microstructures is shown in Table IV. Relevant information gleaned from the corresponding microstructures is as follows.

(a) When the Fe/Mn ratio is close to 2, the β-iron needles cannot be properly distinguished, no matter how slow the cooling rate.

(b) For a 0.76 wt % Fe concentration (with Mn ~ 0.17%), the β-iron phase is not noticeable for DAS

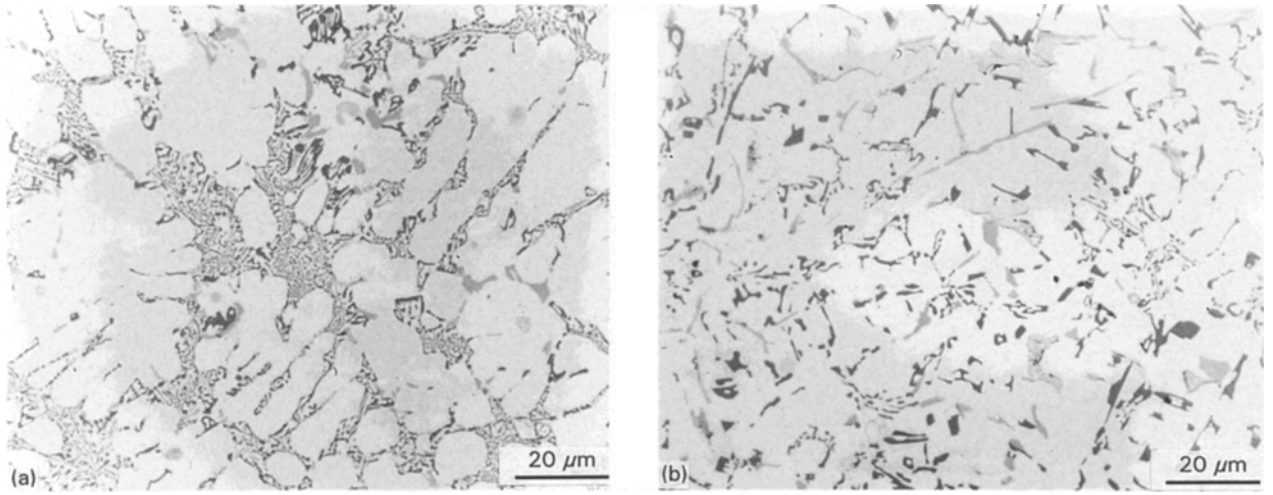

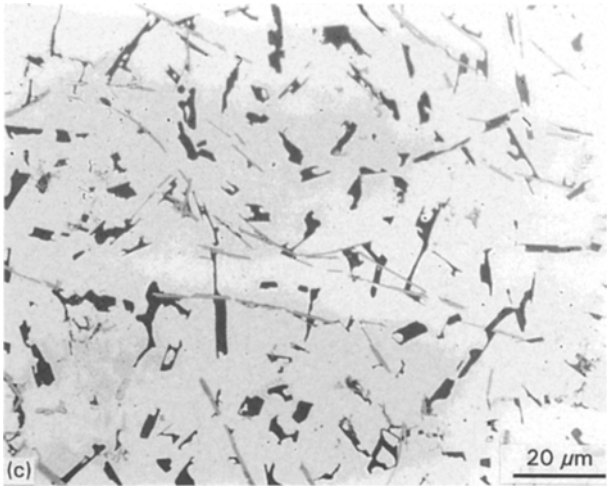

Figure 5 Microstructures of 380 alloy containing different concentrations of iron and cooled at $\sim 260\,^{\circ}C\,s^{-1}$: (a) 0.76 wt % Fe; (b) 1.5 wt % Fe; (c) 1.8 wt %Fe.

TABLE IV Effect of dendrite arm spacing (DAS) and iron content on the size of β-iron needles

Fe conc. (wt %)	Average β-iron needle length (μm)[a]			Maximum β-iron needle length (μm)[a]			Fe/Mn ratio
	DAS: 40–60 μm	DAS: 10–15 μm	DAS: 4–6 μm	DAS: 40–60 μm	DAS: 10–15 μm	DAS: 4–6 μm	
0.76	158.1	31.1	Nil[b]	227.4	56.2	–	4.4
1.0	233.8	53.8	9.9	327.2	88.9	19.3	5.9
1.5	568.5	200.8	15.3	1090	253.4	24.5	8.8
1.8	938.5	217.1	21.3	1326	436.1	36.3	10.6

[a] Average of 40–50 readings.
[b] No β-iron needles observed in the microstructure.

$\sim 12\,\mu m$ or less. It is only detectable in the melt-quenched samples (DAS $\sim 5\,\mu m$) when the iron concentration is of the order of 1.5 wt % or more.

Fig. 6 is the enlarged portion of the solidification curve for various iron contents, corresponding to a cooling rate of the order of $10\,^{\circ}C\,s^{-1}$. As the iron content is increased, a double hump is seen. The iron phases begin to form just below the liquidus temperature, and together with the primary-phase solidification, are the probable cause of this hump [10].

Manganese in small quantities is beneficial in the refinement of the microstructure, particularly when iron is present. The presence of manganese alters the needle-like characteristics of the iron–silicon precipitate to Chinese script, which is much less deleterious to the mechanical properties. It is normally specified in die-casting alloys to a maximum of 0.5 wt %. As manganeses can form a sludge in the liquid state when mixed with iron, it is always considered in relation to iron [15]. In any event, manganese should not exceed half the iron concentration because of the contribution of manganese to sludging. The relationship between the α-aluminium dendrite arm spacings (DAS) and those measured for α-iron phase particles is listed in Table V. The α-iron phase which forms during solidification and the sludge which forms during the

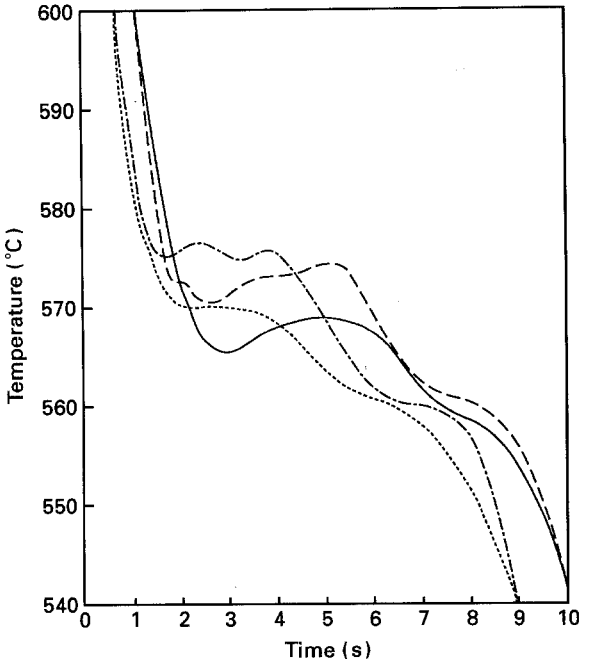

Figure 6 Enlarged temperature–time cooling curves for water-chilled alloys containing different concentrations of iron: (——) 1.30, (- - -) 1.50, (— · —) 1.80, (----) base (1.0) wt %.

TABLE V Relationship between α-aluminium and α-iron dendrite arm spacings

α-aluminium DAS (μm)	α-iron DAS (μm)
40–60	15–20
10–15	1.5–2.0
4–6	0.5–0.7

holding period have the same chemical formula, $Al_{15}(Mn,Fe)_3Si_2$, but vary in morphology.

When the 380 alloy containing 0.46 wt % Mn and 1.01 wt % Fe was solidified at a rate of $\sim 12\,^{\circ}C\,s^{-1}$, sludge occurred in two distinct forms: (a) as small fragments, about 15–20 μm in diameter (some of them having the famous cross-like shape reported for this phase [16]); (b) in continuity with the Chinese script α-iron phase, as shown by the arrow in Fig. 7a. When the same alloy was solidified at cooling rates of the

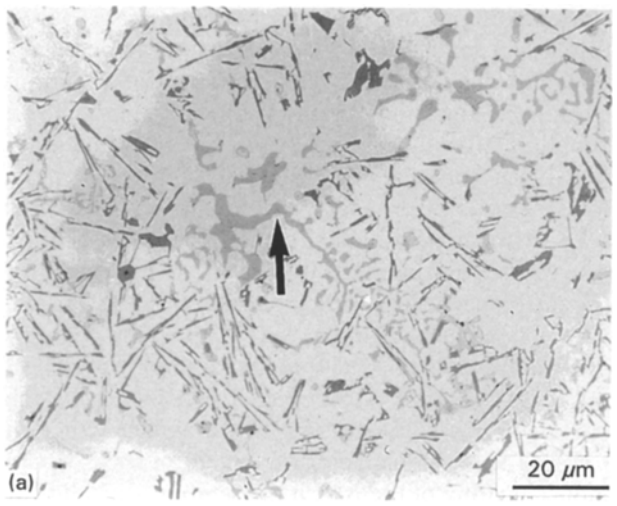

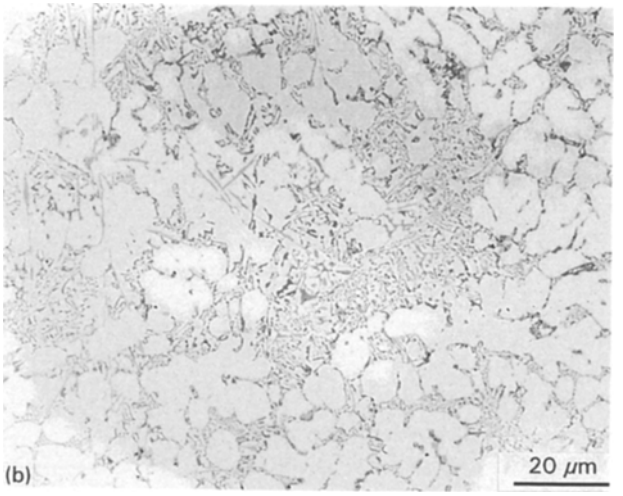

Figure 7 Microstructures of 380 alloy containing 0.46 wt % Mn and 1.01 wt % Fe cooled at (a) $12\,^{\circ}C\,s^{-1}$ and (b) $115\,^{\circ}C\,s^{-1}$.

order of $150\,^{\circ}C\,s^{-1}$ (Fig. 7b) or above, traces of sludge (~ 2 μm) were found widely dispersed in the matrix. Also, Chinese script α-iron phase particles were more frequently observed.

Addition of copper to Al–Si alloys increases their strength and fatigue properties without loss of castability [1]. At the end of solidification process of the 380 alloy, precipitation of Al_2Cu and the more complex eutectic phase $Al_5Mg_8Cu_2Si_6$ takes place [3]. According to ASTM specifications [2], the copper content in the 380 alloy lies in the range 3–4 wt %.

Fig. 8a displays the microstructure of the 380 alloy with 4.09 wt % Cu, cooled at $\sim 10\,^{\circ}C\,s^{-1}$. The copper-bearing phase (Al_2Cu) appears more or less in a blocky form. Because it is the last phase to solidify, it nucleates at the interfaces of other microstructural constituents, namely silicon, α-iron, β-iron phases. At a cooling rate of $\sim 195\,^{\circ}C\,s^{-1}$, the Al_2Cu phase, although still visible in the matrix, occurs in the form of spherical pockets of fine eutectic having diameters ~ 2–4 μm (Fig. 8b, arrowed). Increase in the cooling rate was found to decrease the amount of Al_2Cu formed considerably. It did not, however, eliminate it completely.

Magnesium as an impurity is limited to 0.1–0.3 wt %. Excessive amounts of magnesium decrease the fluidity of molten alloy. Addition of magnesium increases hardness but decreases elongation and impact strength of castings. Magnesium and silicon combine to form the intermetallic compound Mg_2Si, affording a very pronounced improvement in mechanical properties after heat treatment. Al–Mg_2Si is also of the type permitting solution and ageing treatment [8]. In 1973, the allowable magnesium content in 380 alloy was revised from 0.1 wt % to 0.3 wt % [6], mainly to accommodate the increasing quantities of magnesium-containing scrap coming into the secondary market.

At a cooling rate of $\sim 12\,^{\circ}C\,s^{-1}$, the microstructure of 380 alloy containing 0.5 wt % Mg, Fig. 9, reveals the presence of small dark particles between the Al_2Cu crystals, representing the final precipitate of the phase $Al_5Mg_8Si_6Cu_2$ [16]. At higher cooling rates typical of

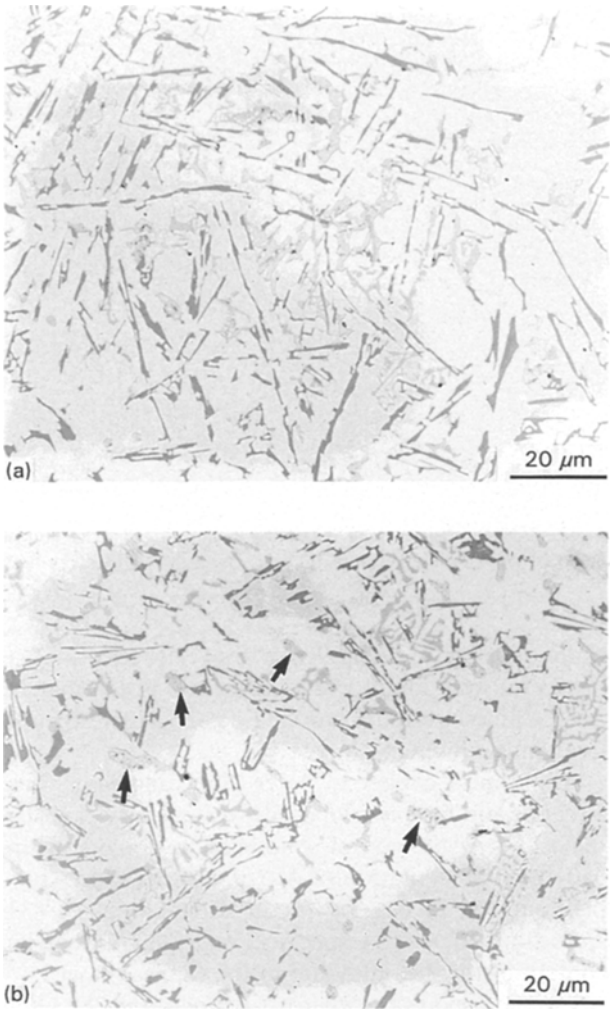

Figure 8 Microstructures of 380 alloy containing 4.09 wt % Cu and cooled at (a) 10 °C s^{-1} and (b) 195 °C s^{-1}.

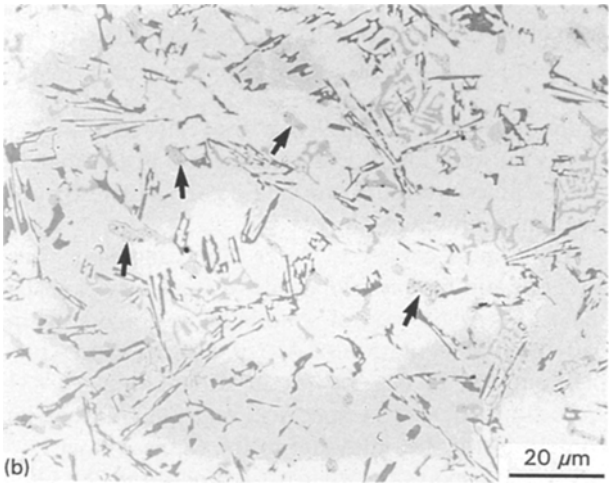

Figure 9 Microstructure of 380 alloy containing 0.5 wt % Mg and cooled at 12 °C s^{-1}.

die casting (~ 100 °C s^{-1} and above), precipitation of magnesium-bearing phases was never observed in the microstructure.

3.3. Effect of heat treatment

3.3.1. Microstructure

The work of Reiso *et al.* [17] on the melting of secondary Al_2Cu phase particles in an Al–4.2 wt % Cu alloy reveals that, after annealing at or above the eutectic temperature, followed by quenching, the eutectic reaction formed in the matrix had a duplex structure that could be resolved in the light microscope. In addition, there was also a small number of particles without internal microstructure (their composition was found to contain 54 wt % Cu, which is exactly the composition of the equilibrium Al_2Cu phase). The melting process of the Al_2Cu phase was explained from the reduction in the Gibbs free energy. The time needed for this melting to occur is very short (~ 1 s). When the nucleation of Al_2Cu is easy (i.e. the Al_2Cu particle is completely melted), the eutectic has the composition of 33 wt % Cu. When nucleation of Al_2Cu is more difficult, the eutectic composition is in the range 35–43 wt % Cu, or even precipitation of one Al_2Cu particle from the enriched melt.

The effect of solution heat treatment (SHT) as demonstrated by the changes in the size and shape of the eutectic silicon particles for solution treatments of 8 h at 480 and 515 °C is summarized in Table VI. In this section, only the microstructures of samples annealed at 515 °C will be discussed.

Fig. 10a represents the microstructure of the present 380 alloy, solidified at ~ 0.3 °C s^{-1}, after solution treatment. Two main observations could be made: (a) the eutectic silicon particles maintain their unmodified morphology; (b) shrinkage cavities form associated with the presence of structureless shiny particles, which were previously Al_2Cu. Higher magnification micrographs, Fig. 10b and c, reveal the presence of fine eutectic rich in copper (as confirmed by energy dispersive analysis of X-rays (EDAX), Fig. 10d) surrounding the silicon particles (Fig.10b), and the structureless shiny particles that are partially or completely melted (Fig. 10c).

Increasing the solidification rate significantly reduces the size of the eutectic silicon particles (Table VI), which, in turn, enhances their spheroidization upon solution heat treatment compared to slowly cooled materials, as for example, the microstructure shown in Fig. 11a, obtained from water-chilled samples. Besides melting of the copper-containing phase, β-iron displays a tendency towards decay through breakdown into ultra-fine particles having a dot-like form. Prolonged annealing at this temperature resulted in complete dissolution of β-iron in the aluminium matrix. In contrast, $Al_{15}(Mn, Fe)_3Si$ in the form of α-Chinese script or sludge was found to persist after such treatment, Fig. 11b. Further increase in cooling rate (melt quenching) resulted in rapid coarsening of the silicon particles during solution treatment, Fig. 12, without passing through the other steps (namely particle breakdown and spheroidization) reported in the literature [18]. It is expected that increasing the cooling rate would shift the Al_2Cu eutectic reaction towards a lower temperature which, in turn, would induce melting of the Al_2Cu phase upon annealing at

TABLE VI Effect of dendrite arm spacing (DAS) on the eutectic silicon particle characteristics of base 380 alloy in the as-cast and solution heat-treated conditions

Condition	Av. particle area (μm^2)			Av. aspect ratio			Particle density ($no.mm^{-2}$)		
	DAS: 40–60 μm	DAS: 10–15 μm	DAS: 4–6 μm	DAS: 40–60 μm	DAS: 10–15 μm	DAS: 4–6 μm	DAS: 40–60 μm	DAS: 10–15 μm	DAS: 4–6 μm
As-cast	110.8	12.3	< 1[a]	2.41	2.58	N/A[a]	557	5503	70647
8 h/480 °C	116.6	6.0	2.15	2.64	2.36	1.82	500	7195	6348
8 h/515 °C	130.5	8.7	2.49	2.66	2.44	1.88	557	5669	7523

[a] The image analyser could not detect the very fine size of the particles individually.

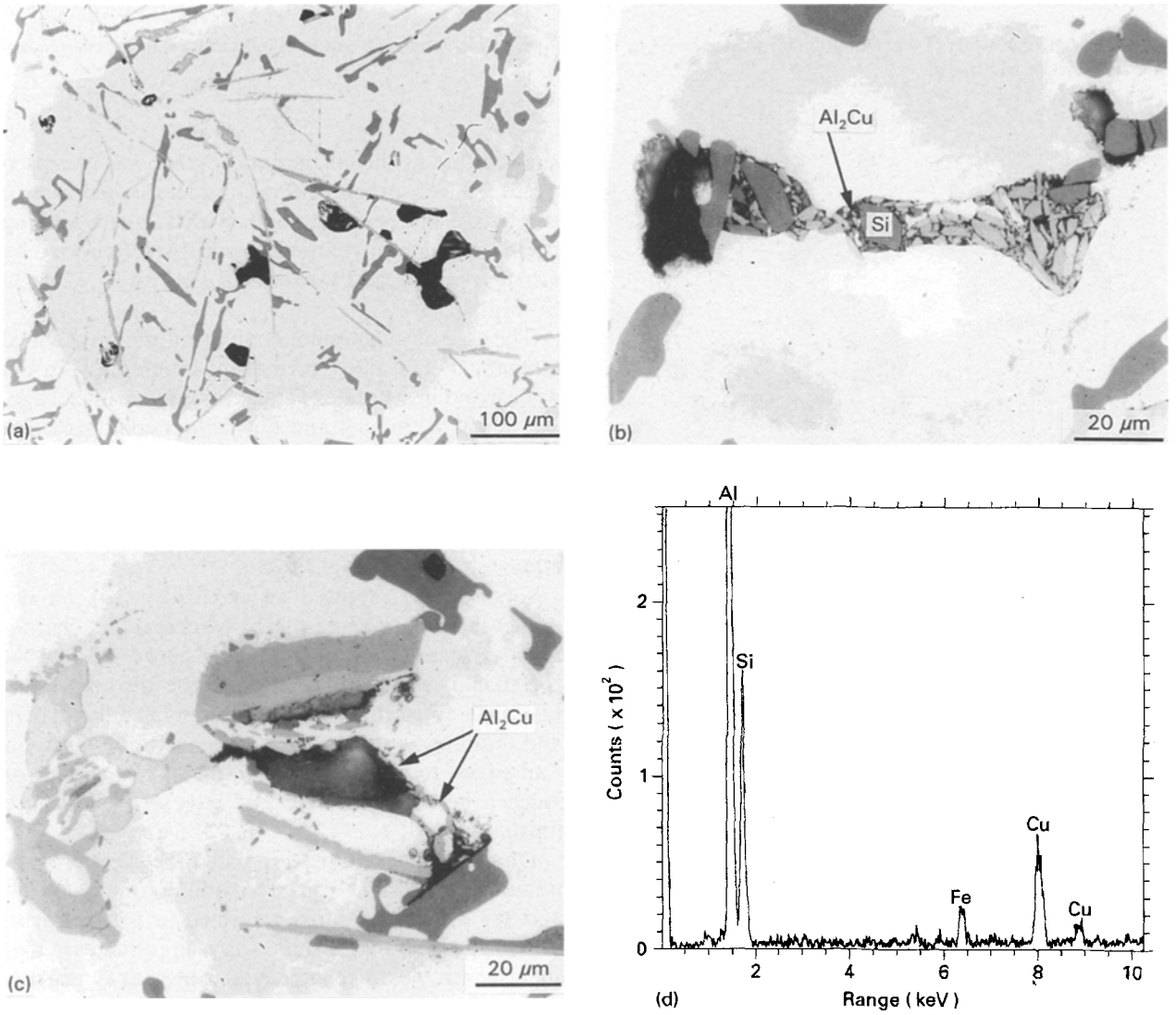

Figure 10 Microstructure of slowly cooled (0.4 °C s^{-1}) 380 alloy, solution treated for 8 h at 515 °C: (a) low magnification showing the persistence of unmodified silicon particles, formation of shrinkage cavities and the presence of structureless phase; (b) formation of fine Al_2Cu eutectic surrounding the silicon particles; and (c) solidification of the melted Al_2Cu phase. (d) EDX spectrometric analysis corresponding to Al_2Cu phase.

515 °C, as is evident in Fig. 12. Table VII shows the hardness of samples solution heat treated (SHT) at 480 and 515 °C, followed by water quenching. No marked difference in hardness of as-cast and SHT samples was noted. This observation highlights the influential role of high solidification rates in maximizing the solubility of alloying elements. Based on this, the as-cast samples were directly aged without solution heat treatment, i.e. T5-tempered.

3.3.2. Hardness measurements

It is well known that pressure die castings cannot normally be solution heat treated (e.g. at 500 °C), because expansion of internal gas porosity can cause the casting surface to blister. With magnesium at its maximum in 380 alloy, a stabilizing anneal at 180–200 °C, over a period of up to 6 h, is reported to result in a progressive hardening of about 10 VPN [6].

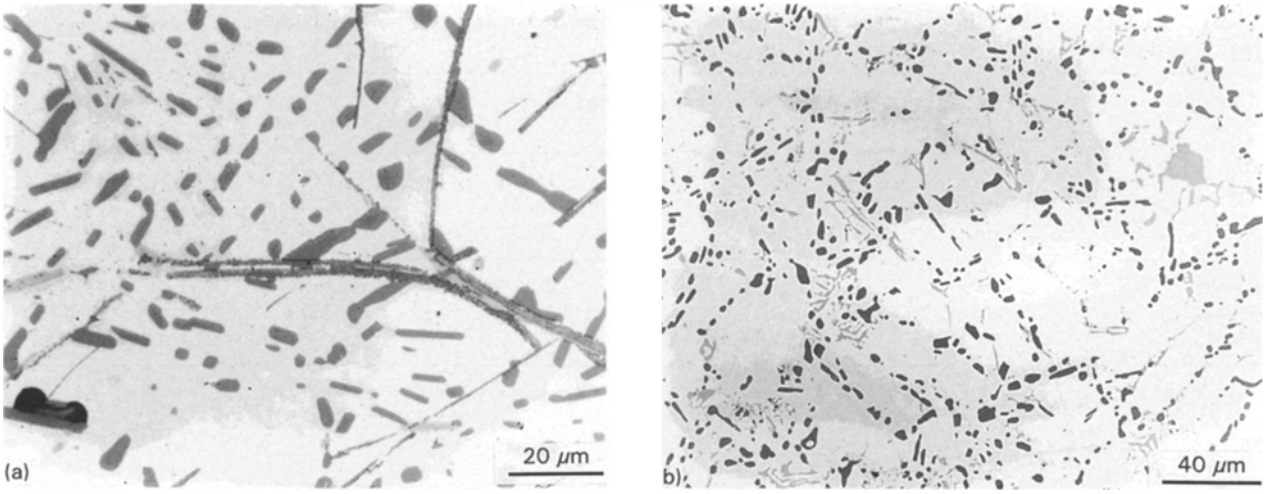

Figure 11 Microstructure of water-chilled alloy treated as in Fig. 10, showing: (a) dissolution of β-iron (needle-like Al_5FeSi); (b) persistence of α-Chinese script and sludge.

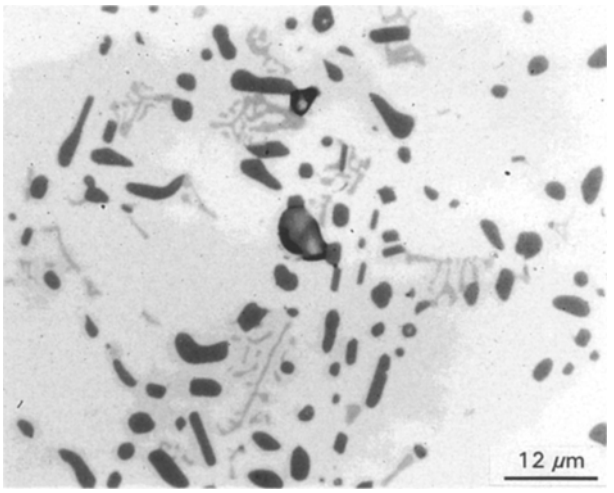

Figure 12 Microstructure of melt-quenched 380 alloy after solution heat treatment revealing coarsening of silicon particles and melting of Al_2Cu phase.

TABLE VII Effect of solution heat treatment on hardness

Mg content of 380 alloy (wt %)	Condition	Hardness (BHN)
0.06	As-cast	86.3
	8 h/480 °C	91.6
	8 h/515 °C	91.3
0.50	As-cast	93.4
	8 h/480 °C	95.4
	8 h/515 °C	96.2

A systematic study was carried out by Harris *et al.* [19] on the effect of magnesium content (0.1–0.6 wt %) on the mechanical properties of a 7 wt % Si alloy produced by permanent mould-casting technique. According to them, there is a wide range of tensile and yield strengths and a comparatively narrow range of elongation that are attainable by varying the magnesium content. In their work, samples were solution treated for 16 h at 538 °C followed by ageing for 4 h in the temperature range 155–205 °C. The results showed that as the magnesium content was increased up to 0.3 wt %, there was a considerable increase in the tensile and yield strength with a corresponding decrease in ductility. Similar results were reported by Ghate *et al.* [20] and Vorren *et al.* [21] on Al–12 wt % Si–Mg alloys.

The role of magnesium content on the mechanical strength of 319 alloy (permanent mould cast) in the as-cast and heat-treated (T5-condition – artificial ageing at 205 °C for 8 h and quenching) conditions has been studied by DasGupta *et al.* [22]. Their work shows that increasing magnesium levels up to 0.6 wt % has negligible effect on the hardness and tensile strength in both the as-cast and heat-treated alloy.

Jorstad [23] reported an extensive study on the influence of magnesium on the machinability characteristics. A small addition of magnesium (~ 0.3 wt %) to 380 alloy was found to improve the alloy machinability. He noted that magnesium hardened the matrix and in doing so reduced the tendency to build up on tool edges, resulted in shorter and tighter chip, provided a better work piece and gave a good surface finish.

Dunn and Dickert [8] compared the effect of magnesium (0.1, 0.35 and 0.55 wt %) on the strength of 380 and 383 die-casting alloys subjected to T5 treatment. The presence of magnesium was seen to increase tensile strength, yield strength and hardness at all temperatures (25–190 °C). Elongation was observed to be reduced by the addition of magnesium. The minimum value, however, appeared to be acceptable, provided the magnesium content was not much higher than 0.35 wt %. According to them, the optimum T5 ageing temperature for these alloys is 4 h at 176 ± 5 °C.

In general, improvement in mechanical properties in magnesium-containing aluminium alloys is attributed to the formation of an age-hardening compound, Mg_2Si, which is precipitated from solid solution during heat treatment. In the as-cast state, Mg_2Si is retained in solid solution, but precipitates as a fine coherent precipitate on heat treatment [24]. Consequently, the presence of magnesium has relatively little

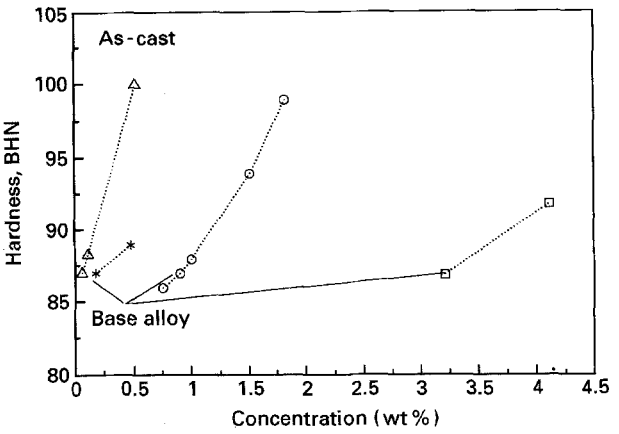

Figure 13 Effect of alloying elements on the hardness of melt-quenched 380 alloy: (○) iron, (△) magnesium, (□) copper, (*) manganese.

effect on the as-cast properties of the alloy. The degree of strengthening depends on the magnesium content. The increase in strength due to higher magnesium content is always accompanied by a corresponding decrease in ductility.

As mentioned previously, the melt-quenched discs, as well as the samples obtained from the other two methods of casting, were mounted in bakelite in order to measure the hardness, and to polish their surfaces for microstructural observations. The mounting process involved heating the specimen together with the bakelite powder to 150 °C in about 9 min, application of a pressure ($\sim 3 \times 10^3$ p.s.i; 10^3 p.s.i $\equiv 6.89$ N mm^{-2}) to mount the specimen, followed by cooling of the mounted specimen to room temperature in about 3 min. Thus the term "as-cast" used in Fig. 13 represents, in reality, hardness measurements made at the end of the mounting process. It is evident from the points plotted in Fig. 13 that increasing the magnesium content in the base 380 alloy up to 0.5 wt % produces the same hardening effect as increasing the iron content from 1.01 wt % to 1.8 wt %, and that this effect is twice that produced by increasing the copper concentration from 3.22 wt % to 4.1 wt %. The hardness value reported by Dunn and Dickert [8] for die-cast 380 alloy containing 0.02 wt % Mg is 81.9 RE ($\sim$ 76 BHN) in the as-cast condition, which increases to 89.7 RE ($\sim$ 86 BHN) when the magnesium content is raised to 0.54 wt %. The slight difference between their results and those shown in Fig. 13 may be explained in terms of the possible precipitation of some Mg_2Si particles during the mounting process.

The combined effect of T5 treatment (4 h at 25, 155, 180, 200 and 220 °C) and alloying elements on the hardness of 380 base alloy is shown in Fig. 14a–d (measured Rockwell F readings were converted to BHN). It can be clearly seen that increasing the magnesium concentration to 0.5 wt % coupled with ageing for 4 h at 180 °C produces the maximum attainable hardening. Though Dunn and Dickert reported only a 7.8 % increase in the hardness of 380 alloy with 0.54 wt % Mg treated similarly, the present simulation shows that this increase could be as high as 30%,

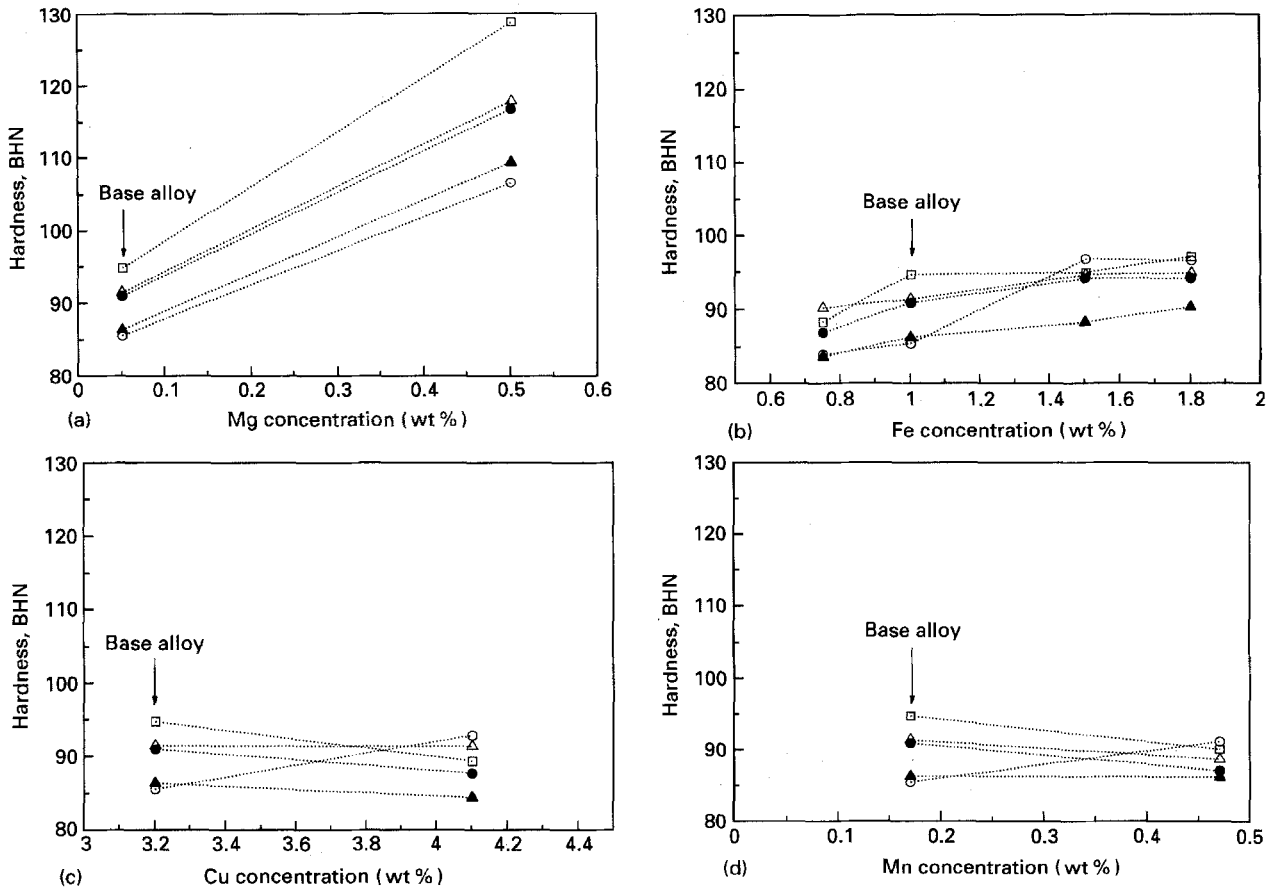

Figure 14 Effect of alloying element on the hardness of melt-quenched 380 alloy in the T5 temper: (a) magnesium; (b) iron; (c) copper; (d) manganese, at (○) 25 °C, (△) 155 °C, (□) 180 °C, (●) 200 °C, and (▲) 220 °C.

Fig. 14a. The difference may be attributed to the cooling rate used to produce the specimens/castings. No microstructural evidence, however, was shown in their work. Therefore, it is rather difficult to estimate the exact cooling rate employed in their study.

It is interesting to note that iron-containing alloys display a somewhat hardening effect upon ageing at 180 °C, Fig. 14b. This observation may be explained in terms of the role of rapid solidification on increasing the maximum solubility of alloying elements, that precipitate later on during the ageing process. The results of Klein [25] reveal that the hardness of copper-containing alloy (2.2 wt %) is about 25 BHN higher than that of non-copper containing alloy. Increasing the copper content from 2.2 wt % to 3.2 wt % increased the hardness further, by about 15 BHN. Although increasing the copper content from 3.2 wt % to 4 wt % increased the as-cast hardness by about 11 BHN, it resulted in softening behaviour when the alloy was aged at temperatures above 155 °C, Fig. 14c. A similar observation was reported when the manganese content was raised to 0.5 wt %, with maximum attainable strength on natural ageing, Fig. 14d.

4. Conclusions

The effect of alloying elements on the microstructure and hardness of 380 type alloys solidified under high cooling rates was studied and the following points were found.

1. At $\sim 260\,^{\circ}C\,s^{-1}$ cooling rate, the β-iron (Al_5FeSi) needles were only detectable at iron levels of at least 1.5 wt % (for an Fe/Mn ratio of 8.8).

2. Increasing the cooling rate (from $0.4\,^{\circ}C\,s^{-1}$ to $\sim 260\,^{\circ}C\,s^{-1}$) considerably decreases the amount of Al_2Cu phase formed, but does not eliminate it altogether. At higher cooling rates, it becomes difficult to distinguish between the fine eutectic pockets and blocky forms of this phase.

3. Magnesium-containing phases (Mg_2Si or $Al_5Mg_8Si_6Cu_2$) are not detectable up to the 0.5 wt % Mg level studied.

4. Traces of sludge ($Al_{15}(Mn,Fe)_3Si_2$) are observed in widely dispersed form even at higher cooling rates ($150\,^{\circ}C\,s^{-1}$ or above).

5. Increasing the cooling rate depresses the solidus line, which permits solution heat treatment at temperatures as low as 480 °C. The α-iron phase characteristics, however, are not affected by the solution treatment.

6. Hardness measurements of as-cast samples (obtained at $\sim 260\,^{\circ}C\,s^{-1}$) show that increasing the magnesium content (from 0.06 wt % to 0.5 wt %) or the iron content (from 1.01 wt % to 1.8 wt %) produces the same hardening effect, and which is twice that obtained on increasing the copper content (from 3.22 wt % to 4.1 wt %).

7. No marked difference in the hardness of as-cast and SHT samples is observed, which emphasizes the influence of high solidification rates in maximizing the solubility of alloying elements (mainly magnesium) in the aluminium matrix, which in turn, considerably improves the alloy strength upon subsequent ageing; the optimum treatment is 8 h at 180 °C, corresponding to T5 temper.

Acknowledgement

Financial support received from the Natural Sciences and Engineering Research Council of Canada is gratefully acknowledged.

References

1. R. W. BRUNER, "Metallurgy of Die Casting Alloys" (SDCE, Detroit, MI, 1976) p. 25.
2. "Metals Handbook," Vol. 15, "Castings," 9th Edn (ASM International, Metals Park, OH, 1988) p. 286.
3. L. F. MONDOLFO, "Aluminium Alloys: Structure and Properties" (Butterworths, London, 1976) p. 759.
4. E. K. HOLZ, "SDCE Trans." (1968) Paper 112, 7 pp.
5. D. L. COLWELL, *AFS Trans.* **60** (1952) 517.
6. E. G. MORGAN, *Foundry Trade J.* 17 June (1982) 887.
7. V. Z. KISUN'KO, E. E. LIKASHENKO, YU. B. BYCHKOV, V. P. EFIMENKO and A. G. MELAKH, *Tsvetnye Metally* (*Sov. J. Non-Ferrous Metals*) **29** (6) (1988) 96.
8. R. P. DUNN and W. Y. DICKERT, *Die Casting Eng.* **19** (March-April) (1975) 12.
9. W. JONSSON, "SDCE Transactions" (1964) Paper 73, 7 pp.
10. S. GOWRI and F. H. SAMUEL, *Metall. Mater. Trans.* **25A** (1994) 437.
11. F. H. SAMUEL, *Metall. Trans.* **17A** (1986) 73.
12. A. M. SAMUEL, H. LIU and F. H. SAMUEL, *Compos. Sci. Technol.* **49** (1993) 1.
13. S, GOWRI and F. H. SAMUEL, *AFS Trans.* **101** (1993) 611.
14. G. GUSTAFSSON, T. THORVALDSSON and G. L. DUNLOP, Metall. Trans. **17A** (1986) 45.
15. "Wabash Aluminum Alloy Data Book". (Wabash Alloys, Wabash, IN).
16. L. BACKERUD, G. CHAI and J. TAMMINEN, "Solidification Characteristics of Aluminum Alloys," Vol. 2, "Foundry Alloys" (AFS/SKANALUMINIUM, 1990, USA).
17. O. REISO, H.-G. OVERLIE and N. RYUM, *Metall. Trans.* **21A** (1990) 1689.
18. F. PARAY and J. E. GRUZLESKI, *Cast Metals* **5** (1993) 187.
19. R. C. HARRIS, S. LIPSON and H. ROSENTHAL, *AFS Trans.* **64** (1956) 470.
20. G. P. GHATE, K. S. SRINIVAS MURTHY and K. S. RAMAN, *Aluminium* **60** (1984) 18.
21. O. VORREN, J. W. EVENSEN and T. B. PEDERSEN, *AFS Trans.* **92** (1984) 459.
22. R. DASGUPTA, C. C. BROWN and S. MAREK, *ibid.* **97** (1989) 245.
23. J. L. JORSTAD, *Soc. Automotive Eng.* (1978) 1.
24. G. K. SIGWORTH, S. SHIVKUMAR and D. APELIAN *AFS Trans.* **97** (1989) 811.
25. F. KLEIN, "NADCA Die Casting Congress and Exposition," 30 September-3 October, 1991, Detroit, Paper T91-033, pp. 59-65

Received 1 June
and accepted 21 September 1994